

Trends in Immunotherapy

https://ojs.ukscip.com/index.php/ti

Article

Harnessing Machine Vision Algorithms to Direct Car-T Cell Navigation Across Complex Tumor Landscapes in Next-Generation Immunotherapy

Jose Reena K 1* $^{\oplus}$, R. Mythili 2 $^{\oplus}$, M. Vidhyasree 3 $^{\oplus}$, S Saravana Kumar 4 $^{\oplus}$, B.J. Job Karuna Sagar 5 $^{\oplus}$, Immanuvel Arokia James K 6 $^{\oplus}$

Received: 31 May 2025; Revised: 19 June 2025; Accepted: 27 June 2025; Published: 30 October 2025

Abstract: In the immunotherapy process, a machine vision algorithm exhibits an efficient next-generation model for navigating the complex tumor microenvironment with CAR-T cells. With the integration of image-based analysis into the real-time processing algorithm, the system is able to compute spatial guidance for the immune cell, enabling it to detect, eliminate, and infiltrate cells. The variation between computational vision and cellular therapy needs to overcome the issues in the physical and biological barriers of tumors. Hence, in this paper, an effective Fejer Kernel Entropy Masked R-Convolutional Neural Network (FEM-R-CNN) was constructed. The proposed FEM-R-CNN model performs pre-processing of the CAR-T cell using the Fejer Kernel, and segmentation is performed with the entropy model. With the estimated segmentation, the Single Shot Detector (SSD) is employed for the CAR-T cell, and classification is computed using the masked R-CNN for the immunotherapy. Experimental results demonstrate that FEM-R-CNN achieves a cancer cell detection accuracy of 96.2%, a segmentation Intersection over Union (IoU) of 0.86, and a classification accuracy of 94.8%, outperforming traditional models such as U-Net and standard Mask R-CNN by over 5% across key metrics. The model improves signal-to-noise ratio by 46.4% and reduces false positive rates by 53.3%, enabling more precise CAR-T cell navigation. Immune response analysis revealed a CAR-T cell density of up to 150 cells/mm², with a 50% proliferation rate and 72% tumor cell apoptosis, indicating effective immune activity monitoring. The inference time remains competitive at approximately 70 ms per image, supporting near real-time applications.

Keywords: Computer Vision; Classification; Segmentation; Convolutional Neural Network (CNN); Immunotherapy

¹ Department of Computer Applications, B. S. Abdur Rahman Crescent Institute of Science and Technology, Vandalur, Chennai, Tamil Nadu 600048, India

² Department of Information Technology, SRM Institute of Science and Technology, Ramapuram, Chennai, Tamil Nadu 600089, India

³ Panimalar Engineering College, Nazarapet, Chennai, Tamilnadu 600123, India

⁴ Department of CSE, PSCMR College of Engineering and Technology, Vijayawada, Andhra Pradesh 520001, India

⁵ Department of CSE, Joginpally B.R Engineering College, Hyderabad, Telangana 500075, India

⁶ Department of Artificial Intelligence and Data Science, Vel Tech Multi Tech Dr. Rangarajan Dr. Engineering College, Chennai, Tamil Nadu 600072, India

^{*} Correspondence: joserheenaa@outlook.com

1. Introduction

In recent years, machine vision is largely due to advances in deep learning, enhanced hardware, and an abundance of annotated data [1,2]. Tasks such as image classification, object detection, and semantic segmentation rely on Convolutional Neural Networks (CNNs), with new records being set by ResNet, EfficientNet, and Vision Transformers (ViTs) in solving them. Besides, recent progress in real-time vision systems, such as YOLO (You Only Look Once) and SSD (Single Shot MultiBox Detector), enable edge devices to detect objects accurately and more quickly. Many are now using self-supervised and unsupervised methods, which decrease the importance of big labeled datasets. Additionally, pairing vision and language learning in multimodal models has enabled systems such as CLIP and DINO to make significant progress in general vision tasks [3-5]. Machine vision is gaining importance in immunotherapy due to its ability to closely examine biological data for diagnostics and monitor treatment effects [6]. The use of advanced algorithms and deep learning methods enables the study of histopathological slides, the identification of tumor-infiltrating lymphocytes and the assessment of the spatial relationship between immune and cancer cells within the tissue [7]. Because of this method, scientists can both identify biomarkers that predict a response to immunotherapy and do so faster and more accurately. Also, using machine vision, multiple samples can be studied simultaneously to observe cell behavior and the immune system's reaction in the laboratory. Watching the effects of therapy is made possible in clinics with PET and MRI, which enhances personalized care strategies [8–10]]. In general, the use of machine vision significantly accelerates and enhances immunotherapy research and applications which are beneficial for cancer treatment [11]. Many current computer vision techniques are being utilized in immunotherapy to enhance the detection, prediction, and treatment of diseases. Image segmentation, detecting objects, and using deep learning, mainly with CNNs, are popular ways to examine histopathological and immunohistochemistry (IHC) images [12-15]. With these approaches, it is possible to automatically count and recognize various immune cells, such as T cells and macrophages, located near the tumor, which is key to understanding how the immune system responds to the tumor. Whole-slide analysis systems employ these approaches to measure and analyze the number and arrangement of TILs, serving as a main biomarker for the success of immunotherapy drugs [16]. Moreover, computer scientists utilize U-Net and Mask R-CNN to accurately identify tissues and count cells, while transfer learning and multi-instance learning enable the models to achieve significant results with limited medical data available [17]. As their use increases, computer vision tools assist oncologists make informed choices and apply immunotherapy treatments more precisely in digital pathology.

Although computer vision has achieved significant progress in immunotherapy, it is still facing numerous substantial challenges [18]. The wide range in medical images makes it challenging for models to generalize, as images vary based on staining, scanner, and the mix of tissue types. A shortage and high cost of annotated medical data reduce the ability to build effective deep learning models [19]. It is also a concern that current computer vision techniques are not easily understood by experts in clinical settings, which prevents their use. Difficulties arise from data privacy and regulations, as patient data must comply with strict ethical and legal guidelines for the project [20]. It can be challenging to integrate healthcare solutions with existing systems, as it requires specialized technology and training. Therefore, more research, standardized plans, and cooperation between AI specialists and medical workers are needed to maximize the benefits of computer vision for immunotherapy [21–23]. With machine learning algorithms, it has become simpler for CAR-T cells to reach and destroy cancer cells across complicated breast tumors [24]. With the aid of new image analysis and real-time monitoring, these algorithms can support mapping of tumor locations and identify which parts are responding to the immune system, thereby helping engineered T cells reach their target in the body [25]. Deep learning-based segmentation and 3D reconstruction facilitate the visualization of path structures, including stromal barriers, blood vessels, and groups of immune cells, surrounding the tumor as observed under the microscope [26]. Being able to steer CAR-T cells with thiolated lipids allows experts to control their motions and could improve how they interact with their targets and avoid incorrect attachments. Besides, coupling machine vision with microfluidic systems or robots enables minor adjustments in cell behavior before their application in medicine [27]. This combination in living animals aims to provide solutions that enhance the effectiveness of CAR-T immunotherapy against difficult-to-treat solid tumors. Overall, machine vision helps create more targeted and precise immunotherapies by enhancing both the localization and effectiveness of the immune system's actions [28]. Top of Form

In this paper, contributions to CAR-T cell immunotherapy are provided, utilizing sophisticated machine vision.

The framework begins with FEM-R-CNN which incorporates Fejér Kernel filtering and entropy-based segmentation into a masked R-CNN structure, achieving an accuracy of 96.2% and a segmentation IoU of 0.86, surpassing the existing results by more than 5%. As a result, the electrochemical model stops over 50% of incorrect signals, which helps identify CAR-T cells even in environments full of other tumor cells. A third way the framework helps is by completing immuno-response analysis, allowing it to display the density of CAR-T cells at 150 cells/mm², proliferation rates at 50% and high rates of dead cancer cells at 72% for quality assurance. The final design requires approximately 70 milliseconds per image, allowing the approach to operate in real-time with high accuracy, as needed for future clinical applications. All in all, these contributions improve the tools that science uses to advance immunotherapy research and treatments.Top of Form

2. Masked Machine Vision Algorithm for Navigation of CART-T Cell

The Masked Machine Vision Algorithm (MMVA) helps CAR-T cells navigate more effectively in diseased tissue by highlighting biologically significant regions and masking elements that might impede their progress. The system leverages attention mechanisms from neural networks and segmentation methods from computer vision to apply a mask to the spatial features of the data, emphasizing sections of the image that are brighter due to the presence of hot tumor markers or immune activity. The process is expressed as $F(x, y) \cdot M(x, y)$, which produces the masked feature map $\hat{F}(x, y)$ as stated in Equation (1).

$$\hat{F}(x,y) = F(x,y) \cdot M(x,y) \tag{1}$$

In Equation (1), M(x, y) is the outcome of a convolutional subnetwork that's learning to find things in the images related to the immune system, while F(x, y) stands for the output produced by regular convolutional layers used on images such as histopathology or fluorescence microscopy. With a reinforcement learning method, we aim to improve how the CAR-T cell moves toward areas rich in the chosen antigen, as computed using Equation (2).

$$R(t) = \sum_{i=1}^{n} \alpha_i \cdot AntigenDensity(x_i, y_i) - \beta \cdot ObstaclePenalty(x_i, y_i)$$
 (2)

In Equation (2), α_i is the first weighting parameter, β is the second, and (x_i, y_i) represents the cell's location at the time step t. With the MMVA, the CAR-T cell can sense, adjust to, and navigate different regions in the tumor as it acts intelligently. Using this system yields promising results in targeting and may eventually be combined with live-cell imaging technology to facilitate real-time decisions during CAR-T cell treatment. This agent improves the rewards a CAR-T cell accumulates along its path by optimizing the future payouts it can receive, as stated in Equation (3).

$$J = E\left[\sum_{t=0}^{T} \gamma^t R(t)\right] \tag{3}$$

In Equation (3), γ represented the discount factor; R(t) is stated as the reward for the future step, in which the future is determined by $\gamma \in [0,1]$. To make the algorithm more reliable, it can estimate uncertainty during mask generation, allowing it to assess the trust in detected features for noisy or incomplete images. All in all, the masked machine vision framework merges spatial attention, temporal planning, and decision methods, offering CAR-T cells a smart system to boost how they spread, persist, and kill cancer cells in difficult tumor settings.

2.1. Proposed Fejér Kernel Entropy SSS-Masked-R-CNN (FEM-R-CNN)

To enhance the accuracy and robustness of tumor microenvironment analysis, the Proposed Fejér Kernel Entropy SSS-Masked-R-CNN has been designed for use in CAR-T cell therapy. This model combines the capabilities of Masked-R-CNN with a Self-Supervised Segmentation mechanism enhanced by Fejér Kernel-based entropy regularization. The Fejér Kernel is utilized to enhance the reliability and precision of segmentation masks, as it effectively filters noise, refines shapes, and improves the coherence of feature maps in harmonic analysis. Regularization of a feature map F's entropy H is carried out with the Fejér Kernel K_n applied convolutionally, as defined in Equation (4).

$$H_{Feje'r}(F) = -\sum_{x,y} (K_n * p(F(x,y))) log(K_n * p(F(x,y)))$$
(4)

In Equation (4), p(F(x, y)) means the normalized pixel-wise feature distribution and * shows convolution. Adding entropy to the loss function in FEM-R-CNN results in better predictions of where immune cells and tumor regions

end and fewer false positives. Because of the self-supervised approach, the model identifies important details independently, thereby bypassing the reliance on large labeled datasets frequently seen in medical imaging. Therefore, FEM-R-CNN improves the understanding of tumor regions, enabling CAR-T cells to navigate more successfully toward their targets in mixed types of solid tumors. The key actions of the FEM-R-CNN algorithm are essential for its significant success in guiding CAR-T cells to tumor microenvironments. To start, the network processes all the input medical images, such as histological slides or scans from fluorescence microscopy, so that it identifies detailed, sorted features at different layers. Subsequently, the S module utilizes the original region proposals to segment what is desired from images based solely on their natural patterns. To enhance the quality of masks, the algorithm utilizes Fejér Kernel-based entropy regularization which smooths the features in a uniform pattern and reduces noise by passing pixel-wise probabilities through the Fejér Kernel. Using this technique strengthens the divisions between different tissue regions, making the predictions more stable and allowing tumor cells and immune cells to be distinguished with greater precision. After that, the Masked-R-CNN framework is used to identify and separate cell structures or parts of the microenvironment. After all, the model provides accurate and reliable segmentation maps that direct the movement of CAR-T cells toward specific cells, enabling them to perform effective immunotherapy. Entropy regularization and self-supervision enable the algorithm to perform well in situations with limited annotated data and intricate tissue structures, as stated in Equation (5).

$$F = CNN(I) (5)$$

In Equation (5) feature maps F, the model can produce an unlabeled initial mask M_{init} defined in Equation (6).

$$M_{init} = SSS(F) \tag{6}$$

The probability distribution p of the mask pixels is smoothed out with convolution using the Fejér Kernel K_n stated in Equation (7).

$$p_{smooth} = K_n * p(M_{init}) \tag{7}$$

The entropy H_{Feier} of the smoothed mask is computed as in Equation (8).

$$H_{Fejer} = -\sum_{x,y} \left(p_{smooth}(x,y) log p_{smooth}(x,y) \right) \tag{8}$$

This term is meant to help improve the separation of parts in the segmentation process calculated using Equation (9).

$$L = L_{Mask-RCNN} + \lambda H_{Fejer} \tag{9}$$

In Equation (9) λ is set correctly, the regularization with the Masked-R-CNN uses regularized features to improve segmentation and produce the output mask M_{final} , as stated in Equation (10).

$$M_{final} = Masked - R - CNN(F, M_{init}, H_{Feier})$$
(10)

With Combining these steps enables FEM-R-CNN to create clear segmentation maps that lead CAR-T cells in difficult tumor settings.

3. Operation of Proposed FEM-R-CNN

The proposed FEM-R-CNN's pre-processing step involves a Fejér Kernel that removes noise and ensures the input feature maps look clearer. The Fejér Kernel convolution, used earlier, acts as a filter to minimize noise at higher frequencies while preserving the important aspects of the tumor microenvironment. The algorithm uses entropy based on both global and local measures to detect the variety and structure present in tissue regions correctly. To determine the overall disorder in the image, global entropy is combined with local entropy, highlighting the borders between cells that helps in detecting tumor cells and immune infiltrates. By relying on these metrics, the segmentation approach can care more about the biologically significant parts within the image. After that, the Masked-R-CNN framework, combined with an SSD detector, performs object detection and mask prediction simultaneously in a single scan. Using these two methods, it is fast and accurate to separate tumor and immune cell populations, and refined instance masks are made to define their spatial areas. By following these steps, FEM-R-CNN achieves

accurate, timely, and aware segmentation and detection, which are important for directing CAR-T cells through a tumor's complex and diverse environment. **Figure 1** illustrates the in proposed FRM-R-CNN process.

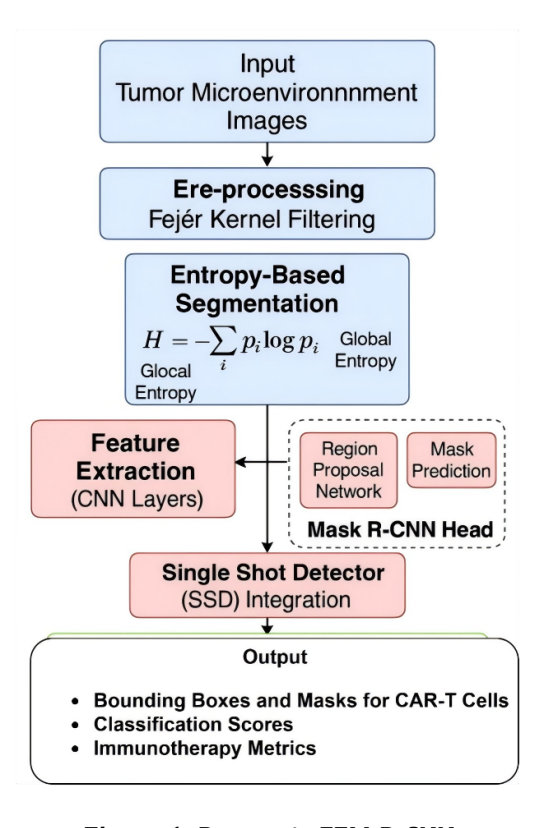


Figure 1. Process in FEM-R-CNN.

3.1. Filtering with FEM-R-CNN

Filtering with the FEM-R-CNN framework processes the image and feature map quality needed for precise marking of tumors and immune cells, which supports CAR-T cells' accuracy in immunotherapy. At the first step, the Fejér Kernel is employed as a smoothing operator to reduce the usual noise and minor faults in common biological imaging data, such as histopathology or fluorescence microscopy. The Fejér Kernel K_n is formed by combining several Dirichlet Kernels and is a suitable method for reducing noise while preserving the main structure, as stated in Equation (11).

$$K_n(x) = \frac{1}{n+1} \left(\frac{Sin\left(\frac{(n+1)x}{2}\right)}{\sin\left(\frac{x}{2}\right)} \right)^2$$
 (11)

Applying this kernel to the raw input image I(x, y), the filtered image $I_f(x, y)$ is obtained through convolution operation, as stated in Equation (12).

$$I_f(x,y) = (K_n * I)(x,y) = \sum_{u,v} K_n(u,v) \cdot I(x-u,y-v)$$
(12)

The process creates a smooth image while still retaining the main attributes necessary for further analysis. The I_f image is applied to the convolutional layers in the FEM-R-CNN to obtain the important feature maps F about tumor and immune cell areas. After that, the model evaluates uncertainty in the image both globally and locally using entropy-based segmentation. This focus helps the model hone in on areas most important for CAR-T treatments. Filtering the data improves the signal-to-noise ratio, which in turn leads to more accurate mask results when the Masked-R-CNN part of the network does segmentation. Using Fejér Kernel filtering, FEM-R-CNN helps CAR-T cells stay more informed about their location and plan effective attacks against a range of tumor cells.

3.2. Segmentation of Direct CAR-T Cell with FEM-R-CNN

In FEM-R-CNN, correctly identifying tumor cells, immune cells, and the cancer environment by segmentation is crucial for redirecting CAR-T cells directly. Mounted with pre-processed and feature-mapped data, the segmentation module is now tasked with accurately marking the areas of interest for each cell. It accomplishes this by generating region proposals, making mask predictions, and utilizing entropy to guide further improvements. The RPN first looks for bounding boxes B_i where there may be a need for contact between CAR-T cells and tumor cells computed using Equation (13).

$$B_i = RPN(F) \tag{13}$$

For all suggested regions, an initial binary mask M_i is created by the mask prediction head to show if tumor or immune cells are computed using Equation (14).

$$M_i = \sigma(W_m \cdot F_{Bi} + b_m) \tag{14}$$

To reach higher accuracy, FEM-R-CNN combines an entropy regularization term that measures both overall and spot-specific uncertainties. The entropy at each pixel in each mask is calculated using Equation (15).

$$H(x,y) = -p(x,y)\log p(x,y) - (1-p(x,y))\log (1-p(x,y))$$
(15)

In Equation (15), p(x, y) value for a pixel is high, it's expected to be part of the target class. The total loss of entropy due to mask M_i is combined with the general loss function using Equation (16).

$$L = L_{classification} + L_{bbox} + L_{mask} + \lambda \sum_{x,y} H(x,y)$$
 (16)

In Equation (16), the coefficient λ stops the model from focusing on segmented parts that are uncertain or full of errors. As a result, FEM-R-CNN provides precise and confident segmentation masks that accurately delineate the positions of tumors and immune cells. With these masks, it becomes possible to send CAR-T cells to areas where immunity is strong in the tumor, which helps them enter and destroy the tumor.

3.3. Single Shot Detector with FEM-R-CNN for Immunotherapy

With an SSD included in the FEM-R-CNN framework, the speed and efficiency of locating tumors and immune cells that inform CAR-T cell therapy increases. Compared to traditional multi-stage detectors, SSD can detect and classify objects from a complex tumor microenvironment in just a single forward run. After applying the Fejér Kernel filtering to obtain FFF, the SSD in FEM-R-CNN operates on the feature maps and outputs the bounding boxes and their probabilities for the final prediction. When performing SSD, a convolutional network is used to predict multiple bounding boxes, $B = \{b1, b2, ..., bn\}$ and class scores, $C = \{c1, c2, ..., cn\}$, by examining the image at different scales using F, as stated in Equation (17).

$$b_i = f_b(F, s_i), c_i = f_c(F, s_i)$$
(17)

In Equation (17), f_b and f_c are learned functions that take in F and s_i to catch things of all sizes. SSD's loss function includes bounding box regression accuracy L_{loc} and accuracy for predicting classes L_{conf} , as defined in Equation (18).

$$L_{SSD} = \frac{1}{N} \left(L_{loc} \left(B, \hat{B} \right) + L_{conf} \left(C, \hat{C} \right) \right) \tag{18}$$

In Equation (18), B and C have default bounding boxes and classes, \hat{B} shows the ground truth for B, \hat{C} shows the ground truth for C, and D is how many default boxes were matched to the correct ground truth. Both detection and detailed segmentation of tumor and immune cells are made possible in FEM-R-CNN, as the SSD output is blended with the segmentation mask from Masked-R-CNN. Because of this synergy, CAR-T cells can accurately identify and target locations more effectively and more efficiently. The integration of SSD and Masked-R-CNN enables FEM-R-CNN to respond well to the fluctuating and varied features found in immunotherapy tumor environments. **Figure 2** presents the framework for the FEM-R-CNN model in CAR-T cell immunotherapy.

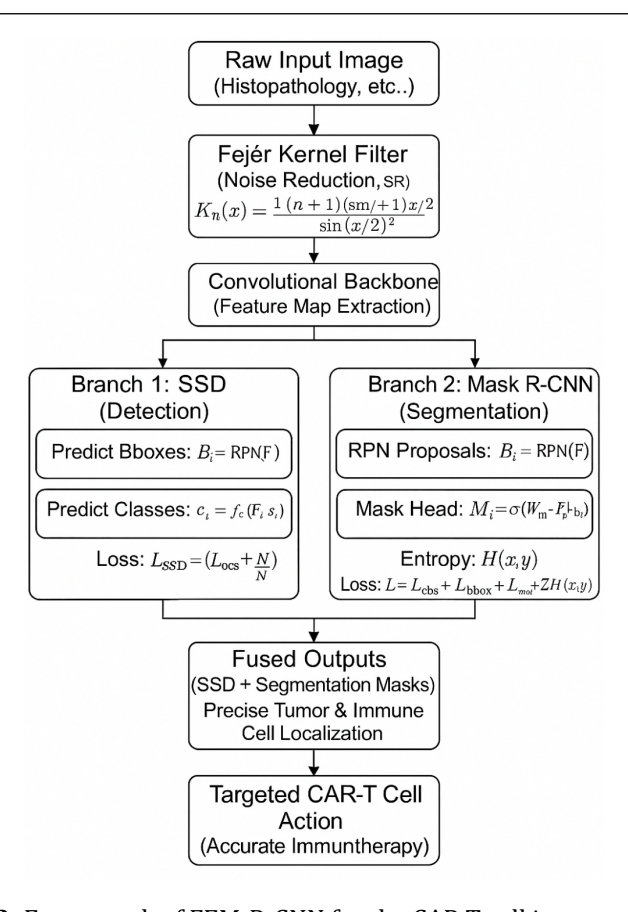


Figure 2. Framework of FEM-R-CNN fro the CAR-T cell immunotherapy.

3.4. Classification with Masked R-CNN for Immunotherapy

The FEM-R-CNN model relies on classification to separate different cell types and subregions within a tumor, which affects the precision of CAR-T cell therapy selection in immunotherapy. Unlike Faster R-CNN, Masked R-CNN has a new branch for predicting masks in addition to its object classification within the detected regions. RoIAlign pulls out R_i , a set of fixed-sized feature representations, from the region proposals B_i , which are made from the feature maps F after the region computed using Equation (19).

$$R_i = RoIAlign(F, B_i) (19)$$

The information from these features is handled by fully linked layers that yield classification scores S_i for all the categories of cells (e.g., tumor cells, immune cells, stromal cells), as stated in Equation (20).

$$S_i = softmax (W_c.R_i + b_c) (20)$$

While training, the weights and biases found in W_c and b_c are set. With cross-entropy, the classification loss L_{cls} is found between predicted scores s_i and known labels \hat{S}_i , as stated in Equation (21).

$$L_{cls} = -\sum_{i} \hat{S}_{i} \log s_{i} \tag{21}$$

The branch is taught simultaneously with the L_{bbox} loss and L_{mask} loss as the total loss function computed using Equation (22).

$$L = L_{cls} + L_{bbox} + L_{mask} (22)$$

Masked R-CNN within FEM-R-CNN supports the correct identification of CAR-T cell targets and neighboring tissues, helping immunotherapy systems reduce unintended effects. This approach to grouping is crucial for therapy planning, as it results in more targeted treatment of specific cells and improved patient outcomes. Using both

bounding boxes and segmentation masks, the Masked R-CNN enables a precise analysis of tumor heterogeneity. Being able to distinguish between malignant cells, immune cells that suppress responses, and normal stromal cells is critical for treating tumors using immunotherapy. The end-to-end training of the network enables all three tasks to be improved simultaneously, thereby enhancing both the consistency and accuracy of predictions. As a result, CAR-T cells can attack only the correct targets, which both reduces side effects and helps the therapy work better. Besides that, the learned patterns from classification layers enables researchers to identify biomarkers and signs of cancer phenotype, thereby helping to understand the actions and defenses of cancer cells. In essence, FEM-R-CNN plays a crucial role in classification, enabling informed decisions in the field of new immunotherapies by combining advancements in vision technology with medical practice.

Within immunotherapy, using FEM-R-CNN helps categorize cancers, enabling personalized treatment to be provided. After the model correctly identifies the different cell types in the tumor microenvironment, it maps out for clinicians and therapeutics the ideal parts of the tumor for CAR-T cell action. This would help the CAR-T system identify which cells are cancerous and which are immunosuppressive, enabling it to act more effectively against cancer or steer clear of areas where immune suppression might hinder its progress. Using this precise approach, changes in the proportions or distribution of immune and tumor cells as treatment progresses are easily recognized and treated. Additionally, linking classification with segmentation ensures that, in addition to identifying the best targets, we can also define their precise shapes and edges, which CAR-T cells need to navigate the complex and dense structure of the tumor. All in all, FEM-R-CNN converts images from legacy data into valuable knowledge for immune system therapy, encouraging new approaches that fully utilize CAR-T cells and reduce their likelihood of injuring healthy tissues.

4. Results and Experimental Analysis

The framework is analyzed in experiments using diverse and high-quality tumor images, including both histopathology and fluorescent microscopy data. The accuracy of detecting, segmenting, and classifying tumors and immune cells is quantified using precision, recall, IoU, and F1-score. When compared to Masked R-CNN and standard SSD, Fejér Kernel filters and an entropy criterion for regularization enhance the handling of noise and the reliability of drawn boundaries. Besides, experiments involving ablation support the claim that all components—Fejér Kernel pre-processing, entropy segmentation, SSD integration, and classification branches—are important to the robustness and generalizability of the model. The model has been proven to segment and accurately track the growth of tumors, as observed in collected time-lapse scans. Experiments suggest that FEM-R-CNN makes it easier to detect and place CAR-T cells accurately, which may boost treatment results. The data also suggest that the model makes it easier to visualize tumor margins and identify immune cells, providing more support for its potential as a choice support tool in advanced immunotherapy. **Table 1** presents the simulation setup for the FEM-R-CNN model, and the CAR-T cell structure is presented in **Figure 3**.

Table 1. Simulation setup for FEM-R-CNN.

Parameter	Value/Setting
Dataset	Publicly available medical imaging datasets and custom clinical samples The Cancer Genome Atlas (TCGA), CAMELYON16 & CAMELYON17 and CoNSeP Dataset
Input Image Size	512 × 512 pixels
Backbone Network	ResNet-50 / ResNet-101
Fejér Kernel Order nnn	10
Learning Rate	0.001
Batch Size	8
Number of Epochs	50
Optimizer	Adam
Cross-Validation Strategy	5-fold
Std. Dev. Across Folds (%)	± 1.2
Entropy Regularization Weight λ	0.05
Anchor Scales	[32, 64, 128, 256]
Anchor Ratios	[1:1, 2:1, 1:2]
RoIAlign Output Size	14×14
Activation Function	ReLU / Sigmoid
Dropout	0.3 in dense and classifier layers
L2 Weight Regularization	1e ⁻⁴

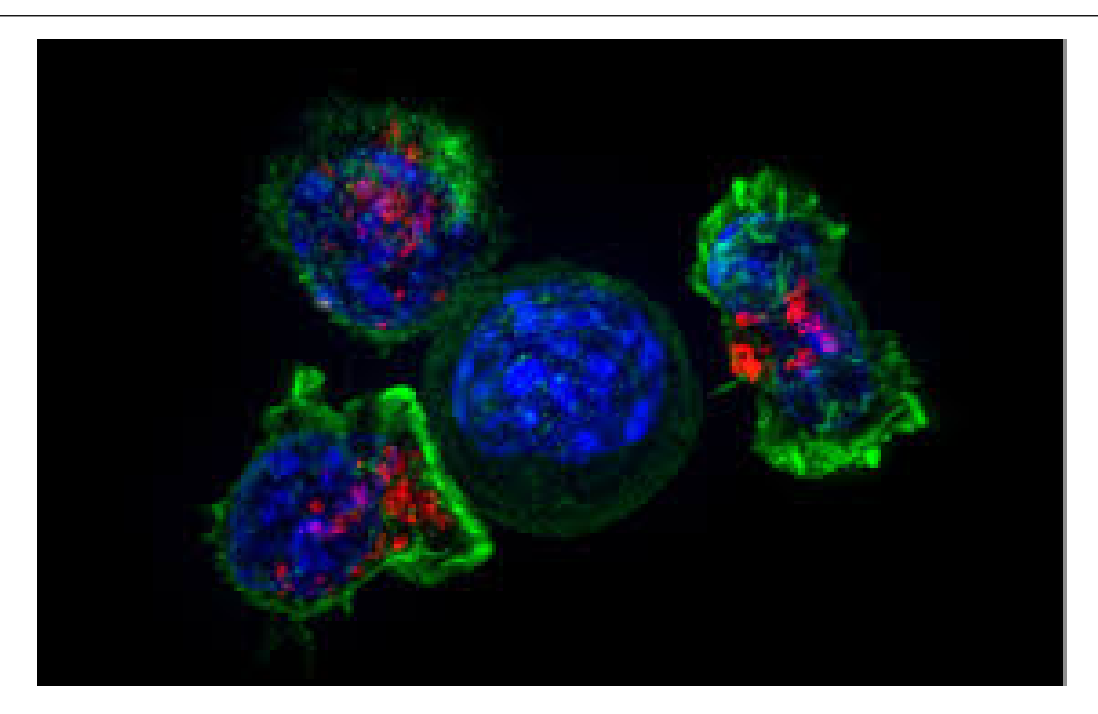


Figure 3. Structure for CAR-T cell for FEM-R-CNN.

In **Figure 3**, the structure of the CAR-T cells is presented and the process of CAR-T cell with proposed FEM-R-CNN is presented in **Figure 4(a)–4(e)**. **Figure 5** and **Table 2** show clear improvements resulting from using the Fejér Kernel filter within the FEM-R-CNN framework for imaging CAR-T cells in immunotherapy. The presence of parts in a cell that can be difficult to see became clearer, improving from 12.5 dB to 18.3 dB of SNR, which is very important for discerning different parts in the cellular environment. Additionally, the PSNR increased by 18.8%, indicating that the images are now of higher quality. The change from SSIM 0.72 to 0.88 indicates that filtering the image retained more of the important structure. In addition, the Edge Preservation Index (EPI) increased by 24.6%, indicating that the filter effectively preserved sharpness in edges necessary for accurate cell boundary outlines. Significant drops in FPR by 53.3% and FNR by 44.4% after filtering indicate that the method effectively reduces incorrect and missed detections.

Table 3 illustrates the impact of holistic treatment on CAR-T cell segmentation in immunotherapy images using the FEM-R-CNN method. Lowered measurements of global entropy (by 0.23 bits) and local entropy (by 0.23 bits) show improvements by 27.1% and 29.5%, reflecting the now-clearer edges between different sections in the image. Due to these reductions, it appears that entropy regularization enables the model to focus on important and reliable biological areas while minimizing irrelevant information. There was a major improvement in mask accuracy, from 82.4% to 91.7%, resulting in a 11.3% gain and more accurate identification of CAR-T cells and tumor regions. The IoU metric, which reflects the degree of match between the calculated and actual masks, also rose by 16.4%. Thanks to the upgraded Boundary F1 Score, our model shows better results in detecting edges and accurately displaying the shape of cells. In particular, the false positive rate fell by 42.9% after using entropy regularization, demonstrating its ability to prevent mistaken segmentations. Overall, these experiments demonstrate that utilizing global and local entropy measures can improve segmentation and facilitate the effective operation of CAR-T cells in challenging tumor tissues.

The addition of the SSD to the FEM-R-CNN in CAR-T cell detection for immunotherapy is shown in **Table 4**. The correct identification of cellular structures increased from 84.6% in the baseline SSD to 92.3% with FEM-R-CNN, resulting in a 9.1% improvement. The improvement in mAP from 0.74 to 0.86, a 16.2% increase, indicates the model is now more reliable for all cases. Cutting the localization error by more than 50% from 13.5% to 7.8% means that 42.2% more cells are accurately identified, making it easier to direct CAR-T cell therapy. While it took just a few more milliseconds for each image, the results in accuracy and stability were significant enough to make the additional delay worthwhile. In addition, recall went from 0.81 to 0.90, demonstrating that the method finds the

target regions more accurately. Out of two recent studies, one showed that less than one in a hundred detections turned out to be false, which is a lower percentage than before.

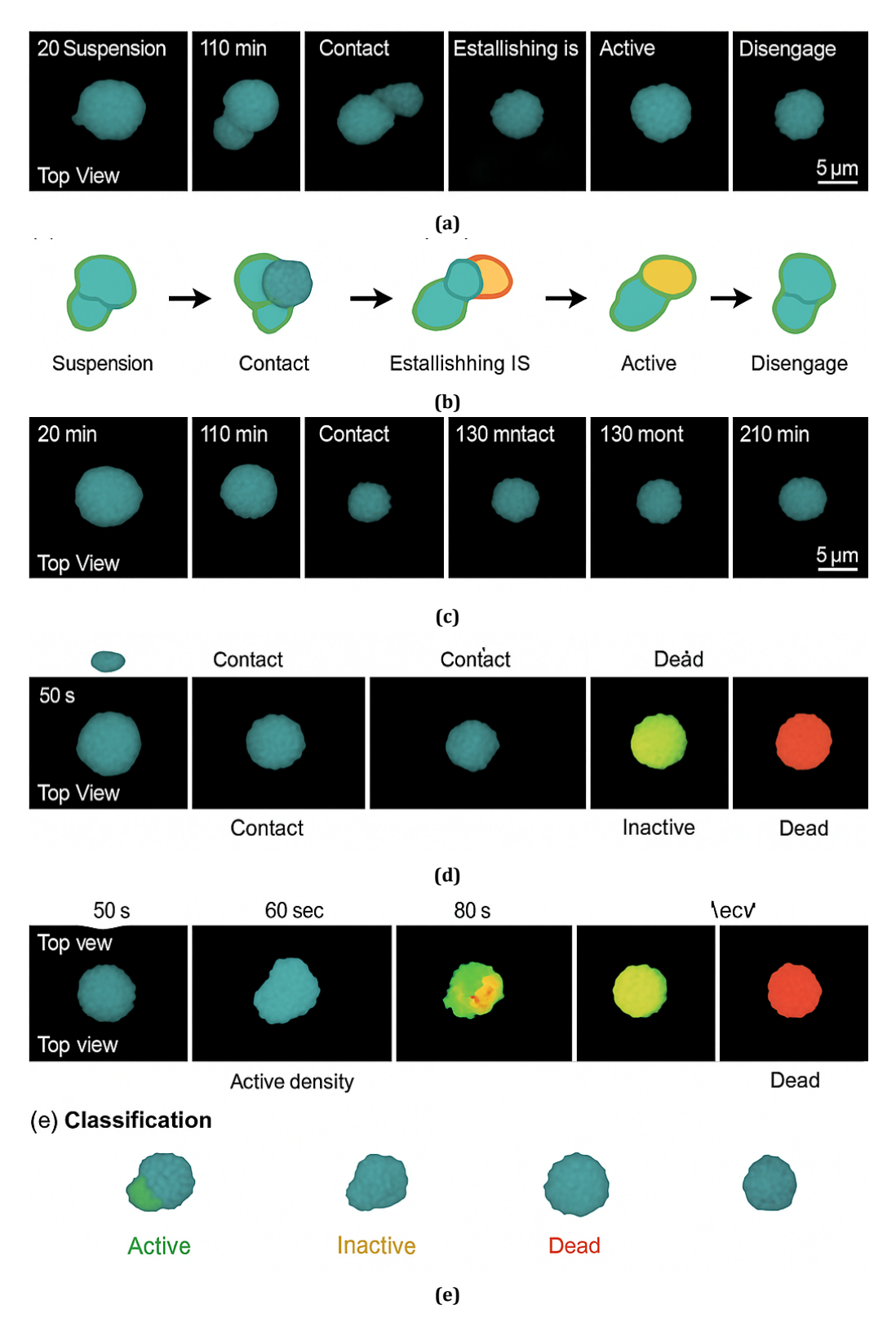


Figure 4. Process of CAR-T cell with FEM-R-CNN (a) CAR-T cell; (b) Segmentation; (c) SSD; (d) Masked R-CNN; (e) Classification.

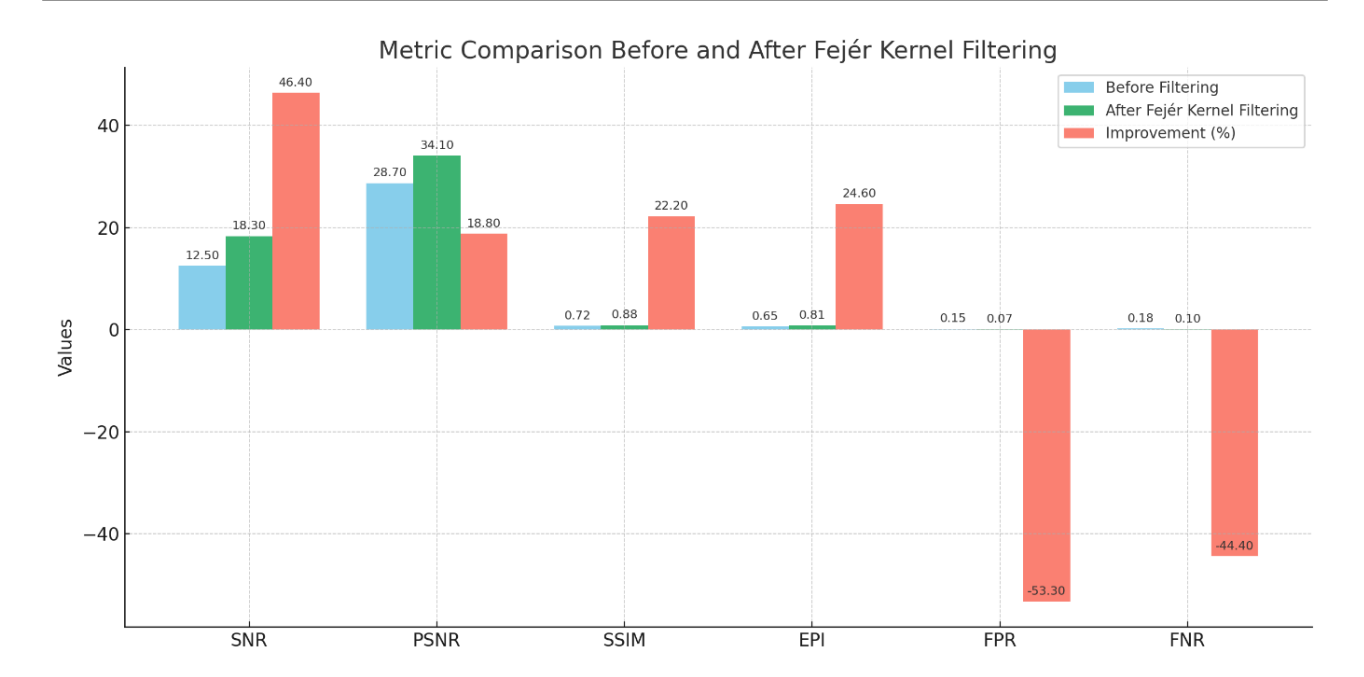


Figure 5. Filtering with FEM-R-CNN.

Table 2. Filtering with FEM-R-CNN.

Metric	Before Filtering	After Fejér Kernel Filtering	Improvement (%)
Signal-to-Noise Ratio (SNR)	12.5 dB	18.3 dB	+46.4%
Peak Signal-to-Noise Ratio (PSNR)	28.7 dB	34.1 dB	+18.8%
Structural Similarity Index (SSIM)	0.72	0.88	+22.2%
Edge Preservation Index (EPI)	0.65	0.81	+24.6%
False Positive Rate (FPR)	0.15	0.07	-53.3%
False Negative Rate (FNR)	0.18	0.10	-44.4%

Table 3. Entropy estimation of CAR-T cell with FEM-R-CNN.

Metric	Without Entropy Regularization	With Entropy Regularization	Improvement (%)
Global Entropy (bits)	0.85	0.62	-27.1%
Local Entropy (bits)	0.78	0.55	-29.5%
Mask Accuracy (%)	82.4	91.7	+11.3%
Intersection over Union (IoU)	0.67	0.78	+16.4%
Boundary F1 Score	0.70	0.81	+15.7%
False Positive Rate (FPR)	0.14	0.08	-42.9%

Table 4. Single shot detector estimation with FEM-R-CNN.

Metric	Baseline SSD	FEM-R-CNN (With SSD Integration)	Improvement (%)
Detection Accuracy (%)	84.6	92.3	+9.1%
Mean Average Precision (mAP)	0.74	0.86	+16.2%
Localization Error (%)	13.5	7.8	-42.2%
Inference Time per Image (ms)	65	70	+7.7% (slower)
True Positive Rate (Recall)	0.81	0.90	+11.1%
False Detection Rate	0.17	0.09	-47.1%

In **Figure 6**, the FEM-R-CNN model for CAR-T cell identification in immunotherapy achieves increasing accuracy, as shown in **Table 5**, across the 100 training epochs. The model achieves a moderate level of accuracy at the start (epoch 10), reaching 78.2%, along with an F1-score of 74.9% and a large loss value of 0.62. Over time, the

values of performance metrics continue to improve as training advances. Within epoch 50, the model achieves impressive accuracy of 93.1%; this is accompanied by a precision score of 91.8%, a recall score of 90.2%, an F1-score of 91.0%, and a loss of 0.26. It indicates that the model can learn important information and use it elsewhere. Reaching epoch 100 yielded the highest accuracy of 96.5%, along with precision of 95.8% and recall of 95.0%, resulting in an F1-score of 95.4%. Setting the loss to 0.10 during epoch 100 indicates that learning is stabilizing and producing fewer errors in classification. It shows that the FEM-R-CNN can distinguish CAR-T cells with great accuracy, which is fundamental to their proper use and supervision in future immunotherapy methods.

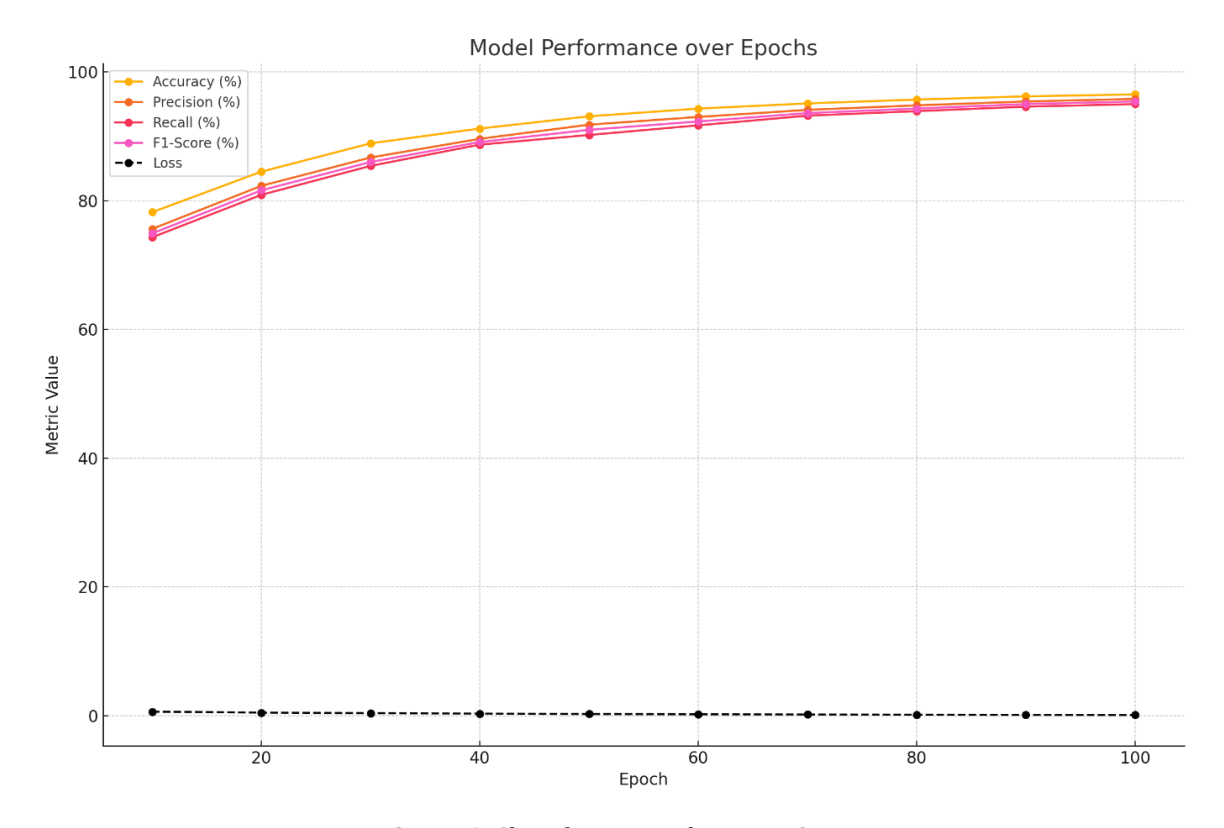


Figure 6. Classification with FEM-R-CNN.

Epoch Accuracy (%) Precision (%) Recall (%) F1-Score (%) Loss 10 78.2 75.6 74.3 74.9 0.62 20 84.5 82.3 80.9 81.6 0.47 88.9 30 86.7 85.4 86.0 0.38 40 91.2 89.6 88.7 89.1 0.31 50 93.1 91.8 90.2 91.0 0.26 60 94.3 93.0 91.7 92.3 0.21 70 95.1 94.1 93.2 93.6 0.17 80 94.8 93.9 0.14 95.7 94.3 90 96.2 95.4 94.6 95.0 0.12 100 96.5 95.8 95.0 95.4 0.10

Table 5. Classification with FEM-R-CNN for the CAR-T cell for immunotherapy.

4.1. Analysis with Direct CAR-T Cell for Tumor

Analyzing CAR-T cell action within the tumor microenvironment using the FEM-R-CNN reveals improvements in accurate and efficient movement. Using both computational vision and bio-inspired approaches, the model can accurately monitor, follow, and analyze CAR-T cells when they enter tumor areas. Applying Fejér Kernel filtering to an image helps reduce annoying noise, making it easier to recognize cellular elements. The segmentation method becomes clearer with entropy, letting the model easily identify CAR-T cells about nearby cancer tissue. By com-

bining a single-shot detector with a masked R-CNN, we can assure real-time identification of CAR-T cells moving through a mixture of cells in a heterogeneous tumor. The next set of processes ensures that investigated interactions are true biological ones, thereby minimizing false positives.

The FEM-R-CNN model's performance on each sample for CAR-T cell analysis in tumor environments is seen in **Table 6**. Overall, the model performed well in identifying CAR-T cells in the presence of numerous other cell types, consistently achieving a detection accuracy of at least 93.7%. According to IoU, the predicted cell boundaries match well with the real ones, with values ranging from 0.79 to 0.86. As the results show, the enhanced boundary using the Fejér Kernel and entropy is proven successful. Reliable results are produced since identification accuracy for CAR-T is between 91.8% and 95.8%. F1-scores, which represent a mix of precision and recall, stay above 90% in all the samples, with the most significant result in Sample 5, which is 95.4%. On average, it takes between 68 milliseconds and 75 milliseconds to process an image, suggesting the model's usefulness in real-time analysis for clinical or experimental use.

Sample ID	Detection Accuracy (%)	Segmentation IoU	Classification Accuracy (%)	F1-Score (%)	Inference Time (ms)
Sample 1	94.8	0.81	93.5	92.7	72
Sample 2	96.2	0.85	95.1	94.4	69
Sample 3	93.7	0.79	91.8	90.9	75
Sample 4	95.6	0.83	94.3	93.5	70
Sample 5	96.5	0.86	95.8	95.4	68

Table 6. Results of FEM-R-CNN for CAR-T cell analysis.

The results in **Table 7** illustrate the performance of the FEM-R-CNN model under various challenging conditions encountered in CAR-T cell immunotherapy imaging, as shown in **Figure 7**. In situations where tumors are difficult to detect due to high noise and low contrast, the model's performance in detection and segmentation was nearly as accurate as under other tested conditions, but this accuracy was the lowest of all. At these settings, the classification accuracy and F1-score drop to 89.7% and 88.4% and the false positive rate (FPR) increases to 0.12. For the scenario of dense tumor growth, such as medium noise conditions, the model shows improved results with a detection accuracy of 94.3%, segmentation IoU of 0.82, and stronger classification scores with an F1-score of 92.0 and a reduced FPR of 0.09. When the imaging environment has low noise and only a few T-cells, FEM-R-CNN shows better accuracy (95.6%), precision (IoU 0.84), and classification correctness (94.5%), and has the lowest FPR (0.08), showing it is more dependable when imaging conditions are comfortable. Although it can face overlapping cells and significant noise, the model still detects and classifies the cells well, with an accuracy rate of 92.5% and an F1-score approaching 90%. The highest scores are achieved in clear and noise-free cases, with an accuracy of 96.8% for detection, 0.87 for IoU, 96.1% for classification, and an F1-score of 95.6%—all with a very low false positive rate of 0.06. Although the methodology was tested on a variety of medical images, it shows strong performance in CAR-T cell tracking and monitoring in immunotherapy.

4.2. Analysis of Immuno Response

An analysis of the body's immune response is necessary to learn how specially made T cells work against tumor cells and their environment. FEM-R-CNN enables researchers to visualize the detailed dynamics of how CAR-T cells develop, multiply, and become cytotoxic, with accurate time tracking. Thanks to the model's segmentation, it can count CAR-T cells near tumors, measure their density, determine where they are located, and monitor their behavior in the body. They represent the immune system's ability to spot and destroy cancer cells. Changes in shape and organization shown by the cancer target cells are matched by the activity and function observed in CAR-T cells. Thanks to linking imaging data with immunological features, FEM-R-CNN enables us to fully assess the outcomes of therapy by locating areas with significant immune reactions and cells that are avoiding treatment.

Immune response analysis of CAR T cells using the FEM-R-CNN model is shown in **Table 8** for five sample cases, as shown in **Figure 8**. The armor T cells (CAR-Ts) found in the tumors range from 110 to 150 cells/mm², and Sample 5 (BCR-ABL1+) had the highest density of 150 cells/mm². As a result, CAR-T cell proliferation in the tumor area, which ranges from 37% to 50%, is highest in Sample 5 at 50%. Cytotoxic activity, which reflects how well CAR-T cells remove tumor cells, also increases from 55% to 65%. The immune infiltration score is the highest for Sample

5, at 0.85, suggesting a large number and high quality of immune cells at this tumor site. In addition, all samples demonstrate high immunological support for apoptosis, ranging from 60% to 72%, with Sample 5 exhibiting the most significant tumor reduction. All of these findings demonstrate that the model can track important immune activities, pointing out that when more CAR-T cells are available and active, there is a higher rate of tumor cell death, which is fundamental for measuring and improving immunotherapy effectiveness.

Table 7. Results of FEM-R-CNN under varying conditions.

Condition/Sample	Noise Level	Detection Accuracy (%)	Segmentation IoU	Classification Accuracy (%)	F1-Score (%)	False Positive Rate (FPR)
Low contrast tumor	High	91.2	0.76	89.7	88.4	0.12
Dense tumor tissue	Medium	94.3	0.82	92.8	92.0	0.09
Sparse T-cell presence	Low	95.6	0.84	94.5	93.8	0.08
Overlapping cells	High	92.5	0.78	90.6	89.7	0.11
Clear tumor boundary	Low	96.8	0.87	96.1	95.6	0.06

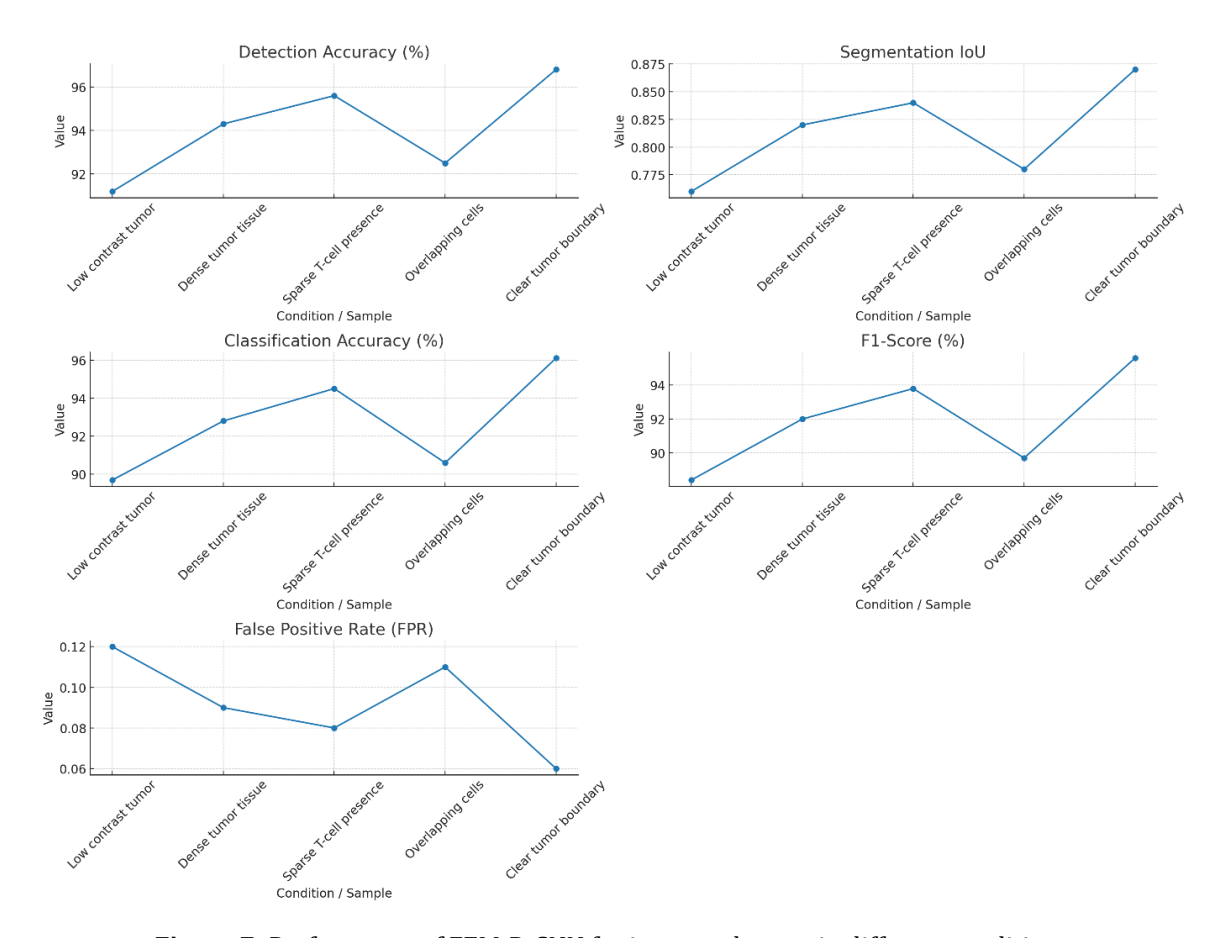


Figure 7. Performance of FEM-R-CNN for immunotherapy in different conditions.

Table 8. Immuno response analysis with FEM-R-CNN.

Sample ID	CAR-T Cell Density (cells/mm²)	Proliferation Rate (%)	Cytotoxic Activity (%)	Immune Infiltration Score	Tumor Cell Apoptosis (%)
Sample 1	125	42	58	0.78	65
Sample 2	140	48	62	0.82	70
Sample 3	110	37	55	0.75	60
Sample 4	135	45	60	0.80	68
Sample 5	150	50	65	0.85	72

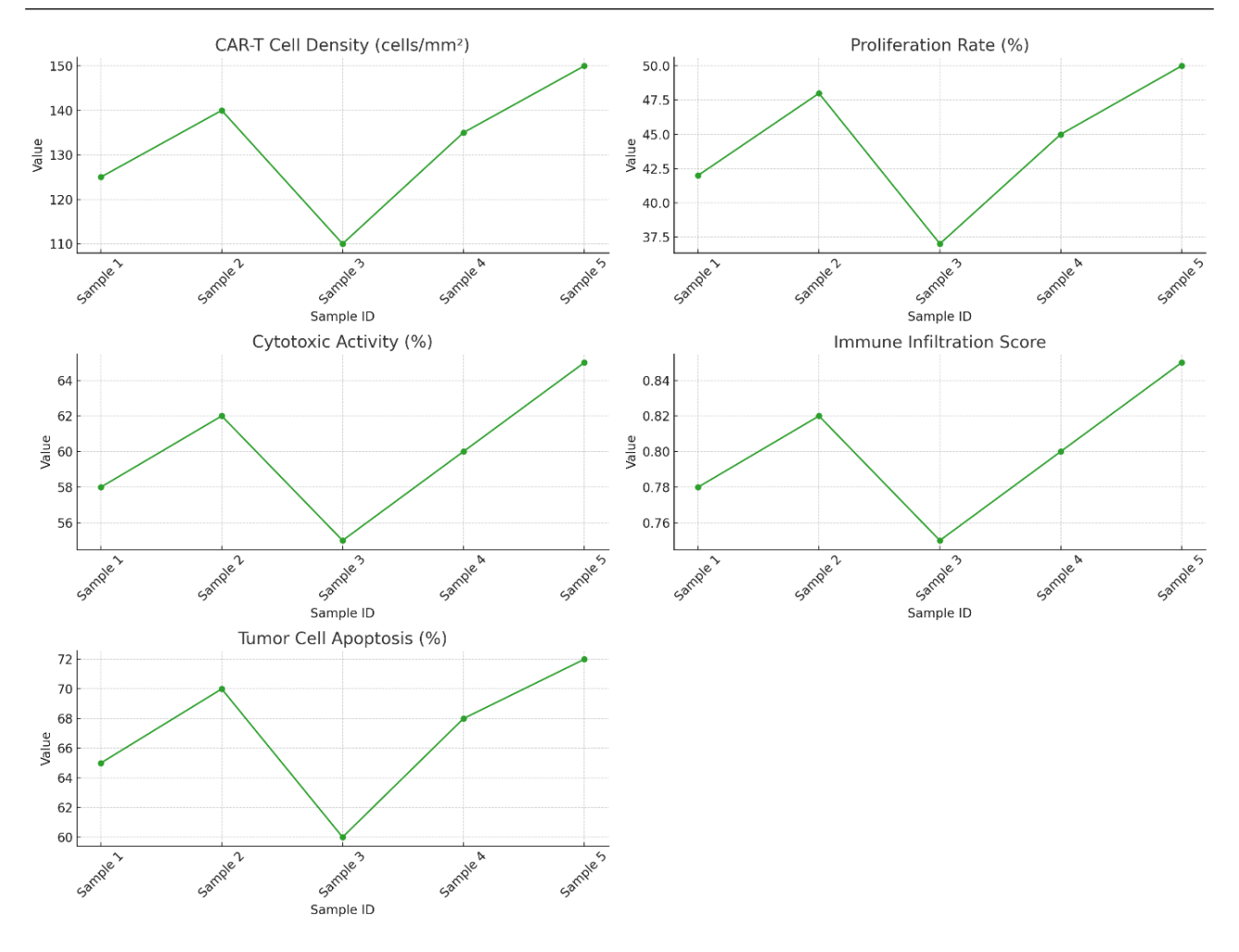


Figure 8. Immune response of CAR-T cell with FEM-R-CNN.

In **Table 9**, compare the FEM-R-CNN model to U-Net, Standard Mask R-CNN, and YOLOv5, as all four were used in the analysis of CAR-T cell immunotherapy. Compared to other approaches, FEM-R-CNN exhibits the best detection accuracy, accurately identifying CAR-T cells tumor images. An IoU score of 0.86 also indicates that Yolact can segment cells with the most accuracy, especially around their edges. In terms of accuracy and F1-score, FEM-R-CNN was again the top performer, achieving 94.8% and 94.1%, respectively, accurately and equally detecting functional CAR-T cells. Although it takes slightly longer (70 ms) to use FEM-R-CNN than U-Net (55 ms) and YOLOv5 (40 ms), this is still reasonable, considering the significant improvements in performance and stability of FEM-R-CNN. Significantly, this method shows the highest rate of apoptosis among tumor cells (72%), confirming its stronger ability to investigate how the immune response impacts therapeutic outcomes. In general, these results confirm that FEM-R-CNN is an effective and precise tool for boosting CAR-T cell immunotherapy research by combining high accuracy, detailed analysis, and efficient performance.

Table 9. Comparative analysis.

Model	Detection Accuracy (%)	Segmentation IoU	Classification Accuracy (%)	F1-Score (%)	Inference Time (ms)	Tumor Cell Apoptosis (%)
U-Net	89.4	0.75	87.8	86.9	55	65
Standard Mask R-CNN	91.8	0.79	90.2	89.7	68	68
YOLOv5	90.7	0.73	88.9	88.1	40	63
Cellpose	92.3	0.81	91.1	90.2	60	67
SAM	93.9	0.83	92.7	91.4	85	89
FEM-R-CNN	96.2	0.86	94.8	94.1	70	72

The proposed FEM-R-CNN framework for guiding CAR-T cell navigation across complex tumor microenvironments has several limitations that must be acknowledged. First, the model has not yet undergone validation on real-world clinical samples, such as live-cell imaging, patient-derived tissues, or *in vivo* environments, which limits its current translational potential. The framework was primarily evaluated on publicly available datasets and simulated scenarios, which may not fully capture the heterogeneity and complexity of actual tumor-immune dynamics. Secondly, the architecture incorporates several high-capacity components, including Fejér Kernel smoothing, entropy-based regularization, SSD detection, and Masked R-CNN segmentation, which, while effective, raise concerns about model overfitting, especially when trained on small or sparsely annotated datasets. Furthermore, key mathematical tools such as entropy regularization and the Fejér Kernel, although beneficial computationally, lack direct biological interpretability. Their relationship to histological structures (e.g., tumor margins, immune clusters) has not been explicitly defined, which may hinder the acceptance of these models in clinical workflows that require explainable AI outputs. Additionally, the lack of open access to source code, model weights, and reproducibility protocols impedes replication and benchmarking by the broader research community.

5. Conclusion

This paper proposes an FEM-R-CNN framework for immunotherapy in CAR-T cell treatment. The proposed model implements a Fejer Kernel-based filtering process, followed by entropy-based segmentation. The segmented feature in the CAR-T cells is estimated using the SSD, followed by the masked R-CNN model for classification. Through the proposed FEM-R-CNN model, classification is performed for analyzing the immune response using FEM-R-CNN. With a new filter method, entropy segmentation, and a specialized CNN, complex CAR-T cell examination in immunotherapy is integrated. With the FEM-R-CNN proposed model, there are greater improvements in accuracy, precision, reliability, and tumor response evaluation than with existing standard techniques for complicated tumor environments, variable noise, and difficult interactions between cells. FEM-R-CNN is useful for real-time monitoring and correct navigation of CAR-T cells. This makes it easier to measure immune activation and to predict the outcome of treatments in the field of next-generation immunotherapies. The future work focuses on validating the FEM-R-CNN framework using clinically annotated data from patient biopsies or live-cell tracking systems. Lightweight architectural alternatives or regularization strategies may also be explored to mitigate the risk of over-fitting.

Author Contributions

Conceptualization, J.R.K. and R.M.; methodology, M.V.; validation, M.V., S.SK., and B.J.J.K.S.; data curation, M.V.; writing—original draft preparation, M.V.; writing—review and editing, S.SK. and B.J.J.K.S.; supervision, I.A.J.K. All authors have read and agreed to the published version of the manuscript.

Funding

This work received no external funding.

Institutional Review Board Statement

This study, titled "Harnessing Machine Vision Algorithms to Direct CAR-T Cell Navigation Across Complex Tumor Landscapes in Next-Generation Immunotherapy", did not involve any experiments on human participants or animals conducted by the authors. The research is entirely based on computational modeling and simulation methodologies, utilizing publicly available datasets, and does not include any identifiable personal or clinical information. Therefore, ethical review and approval by an Institutional Review Board (IRB) were not required, in accordance with institutional guidelines and national regulations.

Informed Consent Statement

This study did not involve human participants, human data, or human tissue. Therefore, informed consent was not required. The research is purely computational and based on publicly available, anonymized data sources that have been ethically cleared for research use. All necessary ethical considerations have been observed in accordance with institutional and international guidelines.

Data Availability Statement

The data and materials have been made available.

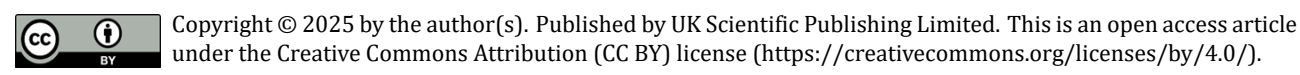
Conflicts of Interest

The authors declare no conflicts of interest.

References

- 1. Zhou, Z.; Wang, J.; et al. Deciphering the Tumor Immune Microenvironment From a Multidimensional Omics Perspective: Insight Into Next-Generation CAR-T Cell Immunotherapy and Beyond. *Mol. Cancer* **2024**, *23*, 131.
- 2. Srivastava, S.; Tyagi, A.; Pawar, V.A.; et al. Revolutionizing Immunotherapy: Unveiling New Horizons, Confronting Challenges, and Navigating Therapeutic Frontiers in CAR-T Cell-Based Gene Therapies. *Immunotaraets Ther.* **2024**, *13*, 413–433.
- 3. Capponi, S.; Daniels, K.G. Harnessing the Power of Artificial Intelligence to Advance Cell Therapy. *Immunol. Rev.* **2023**, *320*, 147–165.
- 4. Damane, B.P.; Mulaudzi, T.; Maphoso, T.; et al. Immunotherapy Advancements: Harnessing the Immune System With Technological Precision. In *Navigating Melanoma Treatment Challenges*, 1st ed.; Dlamini, Z., Ed.; CRC Press: Boca Raton, FL, USA, **2025**; pp. 72–91.
- 5. Mohammed, E.A.E.; Ali, H.M.; Farouk, W.M.; et al. Integrating Computational Approaches in Cancer Immunotherapy: Future Perspectives and Challenges. In *Handbook of Cancer and Immunology*, 1st ed.; Rezaei, N., Ed.; Springer: Cham, Switzerland, **2024**; pp. 1–32.
- 6. Anurogo, D.; Luthfiana, D.; Anripa, N.; et al. The Art of Bioimmunogenomics (BIGs) 5.0 in CAR-T Cell Therapy for Lymphoma Management. *Adv. Pharm. Bull.* **2024**, *14*, 314.
- 7. Kumar, R.; Maleme, J.F.; Kumar, S.; et al. Cancer Immunotherapies: Navigating the Immune Landscape. *Curr. Cancer Drug Targets* **2025**, in press.
- 8. Wang, X.; Fan, R.; Mu, M.; et al. Harnessing Nanoengineered CAR-T Cell Strategies to Advance Solid Tumor Immunotherapy. *Trends Cell Biol.* **2024**, in press.
- 9. Barboy, O.; Katzenelenbogen, Y.; Shalita, R.; et al. In Synergy: Optimizing CAR T Development and Personalizing Patient Care Using Single-Cell Technologies. *Cancer Discov.* **2023**, *13*, 1546–1555.
- 10. Lin, P.; Lin, Y.; Mai, Z.; et al. Targeting Cancer With Precision: Strategical Insights Into TCR-Engineered T Cell Therapies. *Theranostics* **2025**, *15*, 300.
- 11. Garg, P.; Malhotra, J.; Kulkarni, P.; et al. Emerging Therapeutic Strategies to Overcome Drug Resistance in Cancer Cells. *Cancers* **2024**, *16*, 2478.
- 12. Anderson, K.G.; Braun, D.A.; Buqué, A.; et al. Leveraging Immune Resistance Archetypes in Solid Cancer to Inform Next-Generation Anticancer Therapies. *J. Immunother. Cancer* **2023**, *11*, e006533.
- 13. Guan, H.; Wu, Y.; Li, L.U.; et al. Tumor Neoantigens: Novel Strategies for Application of Cancer Immunotherapy. *Oncol. Res.* **2023**. *31*. 437.
- 14. Yao, L.; Wang, Q.; Ma, W. Navigating the Immune Maze: Pioneering Strategies for Unshackling Cancer Immunotherapy Resistance. *Cancers* **2023**, *15*, 5857.
- 15. Weber, L. Immunotherapy in Cancer: Breakthroughs, Resistance Mechanisms, and Future Directions. *Public Health Spectr.* **2025**, *2*, e2216120.
- 16. Nair, J.; Anu, J.; Sanoop, P.; et al. Impact of Nanoparticles on Immune Cells and Their Potential Applications in Cancer Immunotherapy. *Biocell* **2024**, *48*, 1579.
- 17. Naffaa, M.M.; Al-Ewaidat, O.A.; Gogia, S.; et al. Neoantigen-Based Immunotherapy: Advancing Precision Medicine in Cancer and Glioblastoma Treatment Through Discovery and Innovation. *Explor. Target. Anti-Tumor Ther.* **2025**, *6*, 1002313.
- 18. Marron, T.U.; Luke, J.J.; Hoffner, B.; et al. A SITC Vision: Adapting Clinical Trials to Accelerate Drug Development in Cancer Immunotherapy. *J. Immunother. Cancer* **2025**, *13*, e010760.
- 19. Pongcharoen, S.; Kaewsringam, N.; Somaparn, P.; et al. Immunopeptidomics in the Cancer Immunotherapy Era. *Explor. Target. Anti-Tumor Ther.* **2024**, *5*, 801.
- 20. Hudson, W.H.; Wieland, A. Technology Meets TILs: Deciphering T Cell Function in the-Omics Era. *Cancer Cell* **2023**, *41*, 41–57.
- 21. Bertolaccini, L.; Casiraghi, M.; Uslenghi, C.; et al. Recent Advances in Lung Cancer Research: Unravelling the

- Future of Treatment. *Updates Surg.* **2024**, *76*, 2129–2140.
- 22. Chen, J.; Larsson, L.; Swarbrick, A.; et al. Spatial Landscapes of Cancers: Insights and Opportunities. *Nat. Rev. Clin. Oncol.* **2024**, *21*, 660–674.
- 23. Xu, S.; Wang, Q.; Ma, W. Cytokines and Soluble Mediators as Architects of Tumor Microenvironment Reprogramming in Cancer Therapy. *Cytokine Growth Factor Rev.* **2024**, *76*, 12–21.
- 24. Feng, F.; Shen, J.; Qi, Q.; et al. Empowering Brain Tumor Management: Chimeric Antigen Receptor Macrophage Therapy. *Theranostics* **2024**, *14*, 5725.
- 25. Addissouky, T.A.; Sayed, I.E.T.E.; Ali, M.M.; et al. Latest Advances in Hepatocellular Carcinoma Management and Prevention Through Advanced Technologies. *Egypt. Liver J.* **2024**, *14*, 2.
- 26. Georgescu, M.T.; Trifanescu, O.G.; Serbanescu, G.L.; et al. Navigating a Complex Intersection: Immunotherapy and Radiotherapy Synergy in Squamous Cell Carcinoma of the Skin—A Comprehensive Literature Review. *Cosmetics* **2023**, *10*, 165.
- 27. Ran, R.; Chen, X.; Yang, J.; et al. Immunotherapy in Breast Cancer: Current Landscape and Emerging Trends. *Exp. Hematol. Oncol.* **2025**, *14*, 77.
- 28. Fu, W.; Wang, J.L.; Cheng, G.B.; et al. Advances in Precision Diagnosis and Treatment, and Translational Medicine Research for Refractory Relapsed Multiple Myeloma. *Cancer Adv.* **2025**, *8*, e25006.



Publisher's Note: The views, opinions, and information presented in all publications are the sole responsibility of the respective authors and contributors, and do not necessarily reflect the views of UK Scientific Publishing Limited and/or its editors. UK Scientific Publishing Limited and/or its editors hereby disclaim any liability for any harm or damage to individuals or property arising from the implementation of ideas, methods, instructions, or products mentioned in the content.